Chapter-4

Coastal urbanization and associated risk

4.1. Impact of tidal fluctuation

In the global and regional scenario of Sea Level Rise (SLR), the sea level is rising at the rate of 2.2 – 3.1 mm/y in the northern Bay of Bengal (Kusche et al., 2016). The Relative Sea Level Rise (RSLR) has resulted from the mutual effect of SLR and vertical land subsidence (Milliman et al., 1989; Church et al., 2006; FitzGerald et al., 2008; Akter et al., 2016). The land is subsided about 1.3 – 7.1 mm/y rate in that region of the Bengal delta (Jana, 2020). Therefore, the altimetric SLR has resulted at the rate of 6.1 mm/y over the period during 2000-2004 (Kusche et al., 2016). In the Bengal Basin, the past RSLR has been estimated as 8-18 mm/y considering the tide gauge data from 1932 to 2005 which even reached up to 25 mm/y rate (Ericson et al., 2006; Kusche et al., 2016). The Sea Surface Temperature (SST) and water salinity are rising at a perilous rate (Kusche et al., 2016). With due effects, the regional SLR will be higher than the present rate.

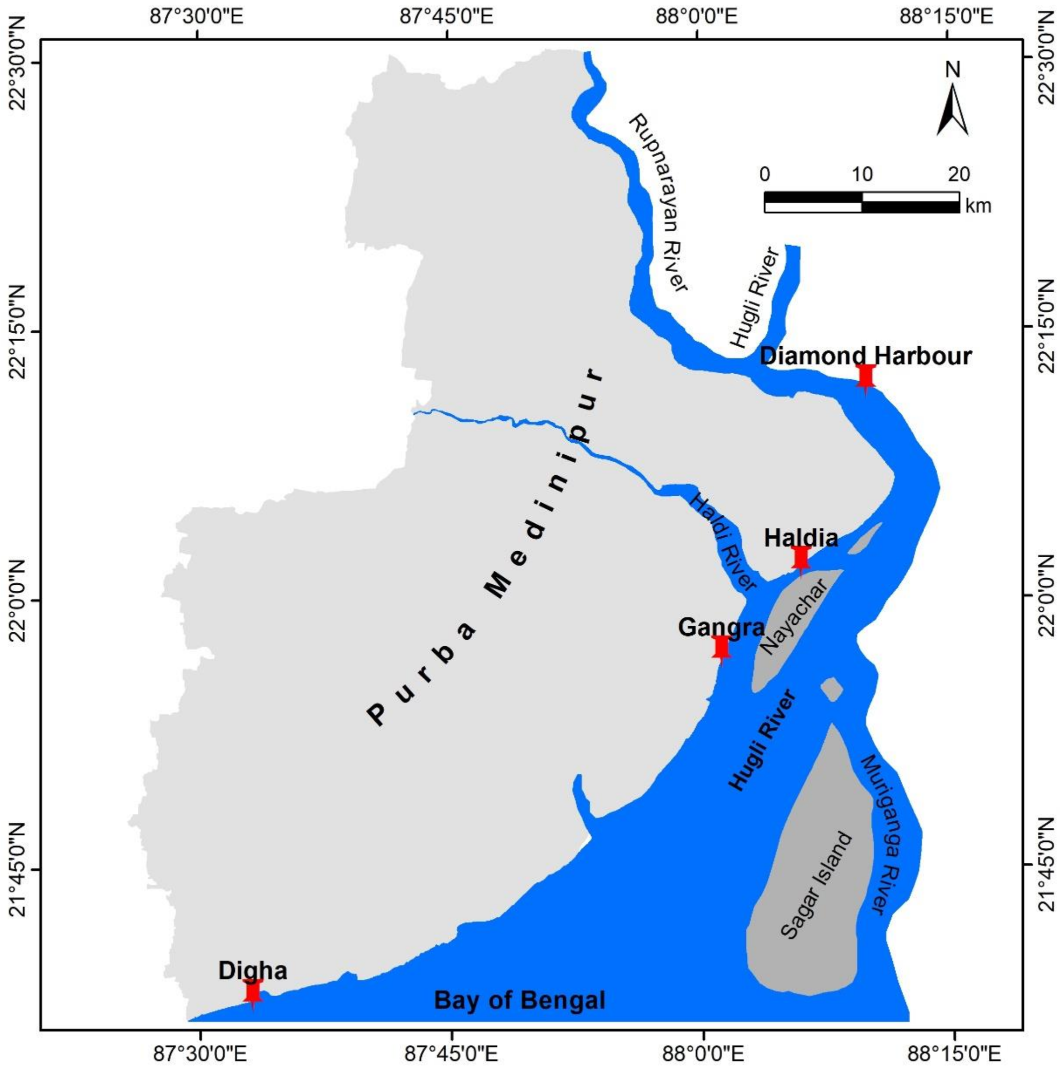

Fig. 4.1: Tide gauge stations around the shoreline of Purba Medinipur coast (Bay of Bengal and Hugli estuary).

The entire coastal region is experienced as meso-tide (2 – 4 m) variation with the mean tidal range of 4.38 m (Jana, 2020). Four tide gauge stations exist around the shoreline of Purba Medinipur coast within the Bay of Bengal (Digha) and Hugli estuary (Gangra, Haldia and Diamond Harbour) (Fig. 4.1). With due effects from the regional and local SLR, the tidal impacts will also be increased in the coastal zones. The tide gauge data of Diamond Harbour during 1948 – 2014 reveals an increasing trend (0.85) of tide level with the highest (7230 mm) and lowest (6883 mm) tide level respectively in the year of 2013 and 1963 (Fig. 4.2a). At Haldia gauge station, the analysis result of available data (from 1971 to 2014) shows a positive (rising) trend (0.73) of tide level with the highest (1750 mm) and lowest (6918 mm) during 2013 and 1972 respectively (Fig. 4.2b). A relatively lower trend (0.34) of rising tide level is observed at Gangra station during 1974 – 2006, where the maximum (7039 mm) in the year of 2000 and minimum (6874 mm) during 1997 (Fig. 4.2c). These three stations reflect the relative increase of tide level at the Hugli estuary. The tide level in Digha reflects the open coastal environment of the Bay of Bengal with a higher trend (0.82) of increasing tide level during 1977 – 2012 with the maximum (5344 mm) and minimum (1655 mm) tide level in the year of 1999 and 1992 respectively (Fig. 4.2d). The overall result clearly indicates the increasing trend of tide level all along the Medinipur coastal stretch.

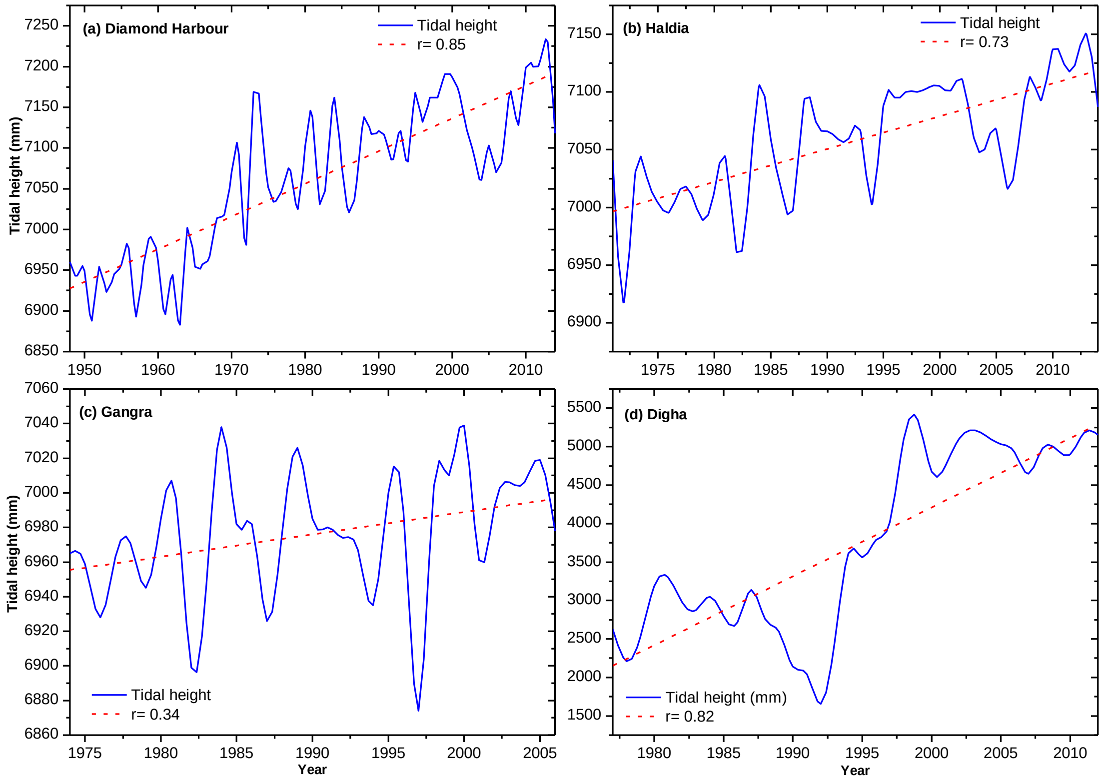

Fig. 4.2: Fluctuation of mean tide level at (a) Diamond Harbour, (b) Haldia, (c) Gangra and (d) Digha gauge station during (a) 1948 – 2014, (b) 1971 – 2014, (c) 1974 – 2006 and (d) 1977 – 2012 (showing the increased vulnerability of tidal elevations towards the low-lying areas of coastal urban centres).

The increasing tide level creates a severe impact on the shoreline and interior parts of the coastal zone. During high tide, Mandarmani coastal zone has been severely affected and tidewater entered into the existing hotels at the seafront positions (Plate 4.1). Waves are repeatedly acting landward side and eroding the shorefront sand dunes and other coastal landforms (Plate 4.2). The saline seawater encroached into the far elevated coastal landforms and the natural coastal habitats which are significantly affected by saline water. The life-supporting occupations of the coastal stakeholders are severely affected due to land erosion and saltwater inundation, and that will be tremendously increased in the near future.

Plate 4.1: Tidewater entered into the hotel during high-tide at Mandarmani coastal belt.

4.2. Water-logging and inundation

The Digha and Haldia urban centres have been existed over the fluvio-marine depositional environment comprising with sand dunes and natural levees in the shorefront and estuarine margin areas. The interior land surface is relatively lower elevated than the seafront part in these two sites. Also, the coastal stretch is segmented by the tidal inlets and creeks. Therefore, the tidewater enters into the interior lowlands and inundates the entire low-lying areas bi-diurnally. The Contai municipality area is situated in the inland dune ridge surrounded by the lowland surface of the swale topography. The tidewater cannot enter up to that area, therefore, tidal inundation is not a problem in that area. However, the storm rainfall can create a water-logging problem in the low-lying areas on both sides (north and south) of the Contai dune.

4.2.1 Tidal inundation at Digha

Ten transects in across the shore (P1 – P10) at about 2.8 km equal spatial interval have been demarcated (Fig. 4.3) and their respective micro-zonation of surface morphometry (Fig. 4.4) have been analysed in Digha coastal stretch to assess the impacts of tide inundation. The micro-zoning cross-profiles have been drawn from the seashore (south) to inland side (north).

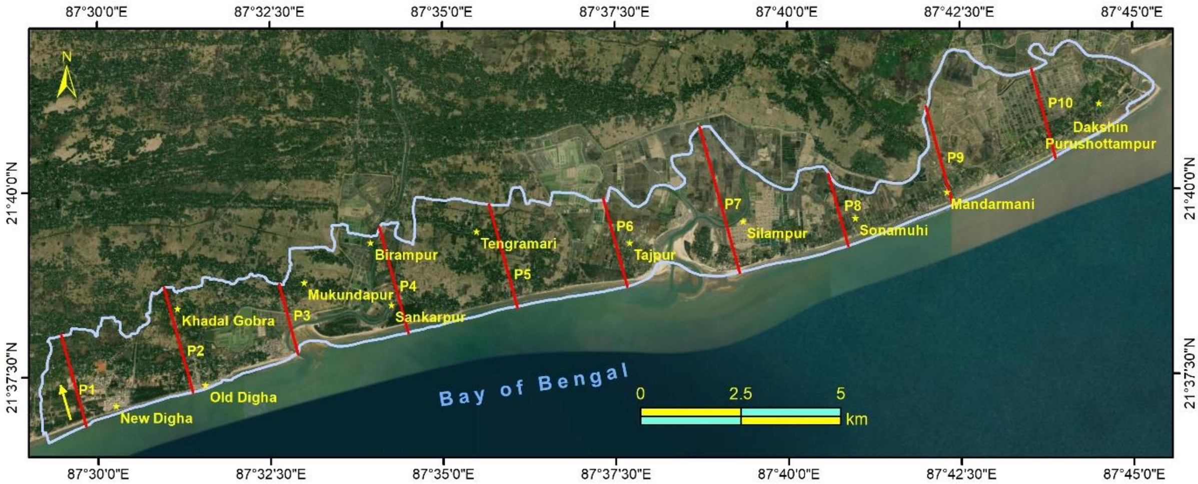

Fig. 4.3: Location of shore-across transects of Digha urban centre.

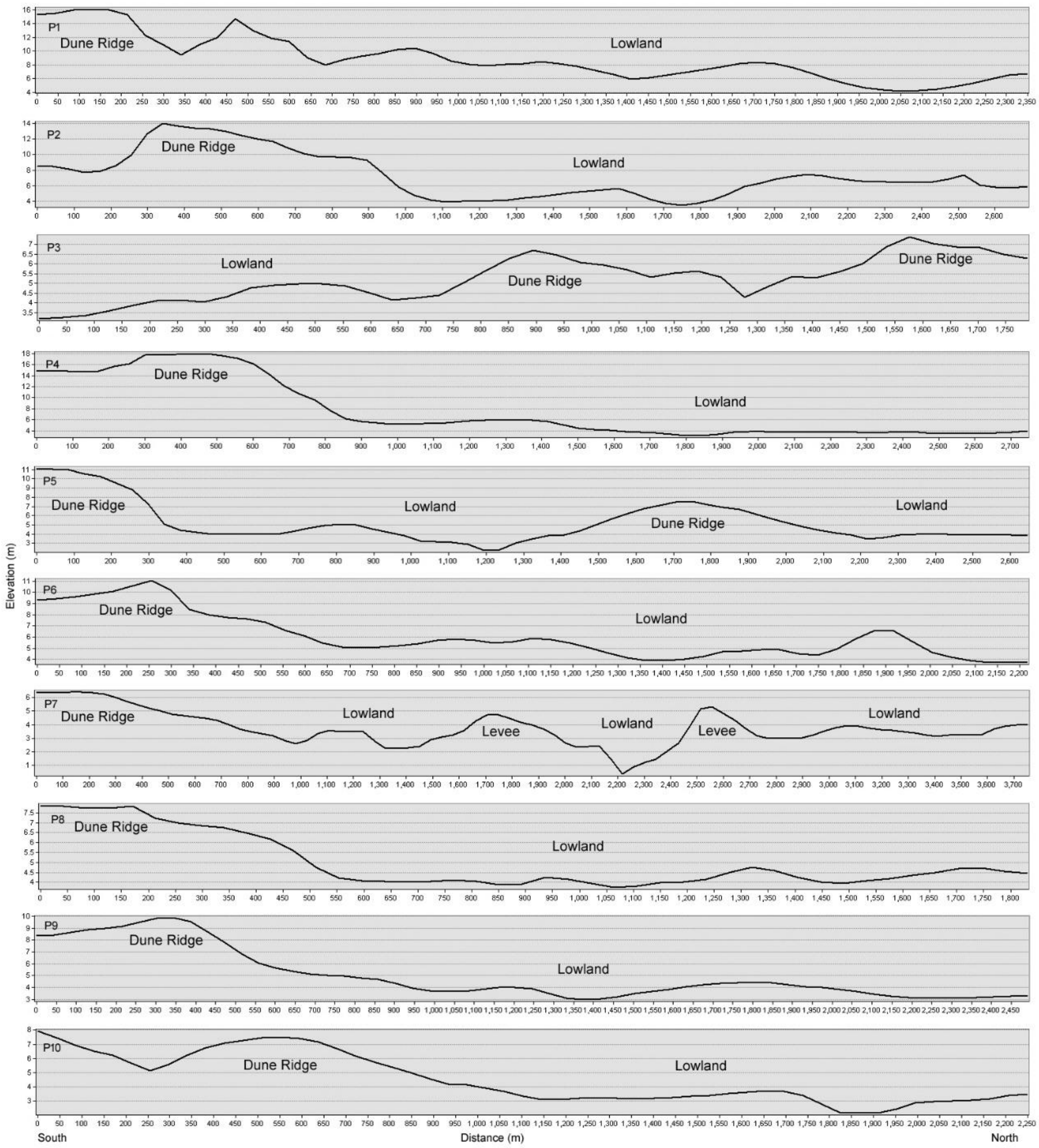

Fig. 4.4: Micro-zonation of surface morphometry along the different transects at Digha.

Among the ten profiles, only the P1 has been demarcated along the Champa rive mouth in the shorefront part, and others are demarcated across the shorefront sand dune. The morphometry of the cross-profiles indicates that the surface elevation is gradually lowered down towards the interior land (except the P3) (Fig. 4.4). The higher slope is observed just after the dune ridge in the landward sides of the cross-profiles. Moreover, the contour pattern and elevation variation indicate the micro-terrain configurations of the coastal stretch (Fig. 4.5).

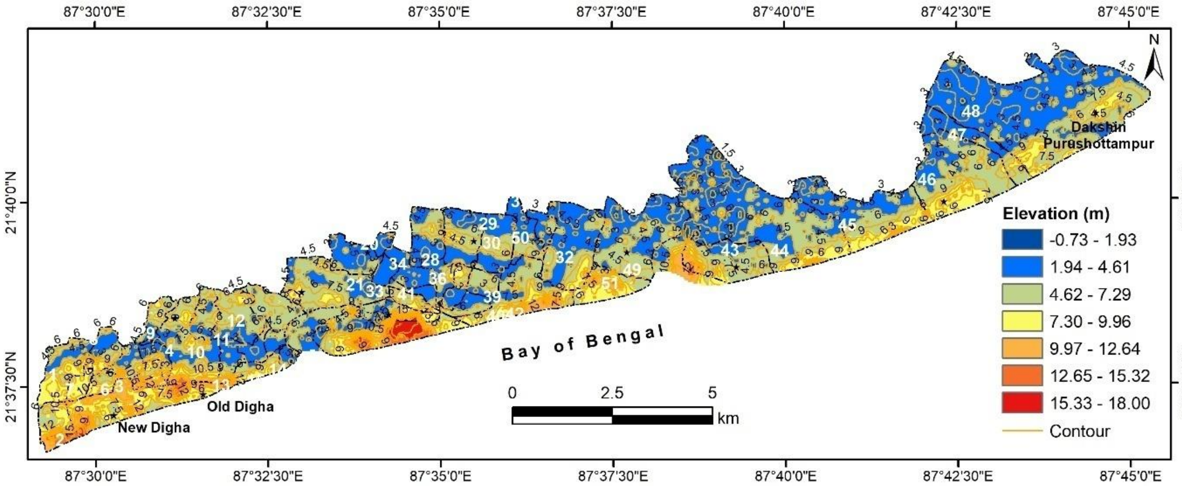

Fig. 4.5: Water logging and saltwater inundation prone areas at Digha urban centre.

Plate 4.2: Shorefront sand dunes are severely eroded at the different sites of Mandarmani-Sankarpur coastal stretch.

The tidal range in the meso-tide-dominated environment at the Digha coast faced a severe problem in terms of coastal inundation. Concerning the 4.61 m tidal amplitude, the inundation zones have been demarcated for the Digha coastal stretch (Fig. 4.5). The tidewater inundation zone shows that about 48 % land area (32.45 km²) of the total area (67.04 km²) will remain under tidewater. Different types of land use and land cover (LULC) classes have existed (Fig. 2.14) within the entire inundation zone. Mainly, the agricultural land and vegetation areas are affected by such kind of saltwater inundations which will be further intensified in the near future. However, it will be beneficial for the aquaculture practices in the wetland areas. Moreover, the recent trend of urban expansion in the low-lying areas (after lowland filling) can severely endure from the predicted tidewater inundation level.

4.2.2. Water-logging at Contai

The Contai municipality area has not suffered from the water-logging problem due to its elevated dune landscape. However, the urban areas have been extended over the lowland areas in the recent time. These settlements of the lowland areas are prone to water-logging and associated problems during the monsoonal storm rainfall events. The six cross-dune transects (P1 – P6) have been demarcated at about 950 m interval (Fig. 4.6) to identify the micro-terrain characteristics. The surface morphometry along the cross-profiles have been demarcated from south to north direction (Fig. 4.7) which shows the relatively elevated dune ridge at the middle part of the cross-profiles.

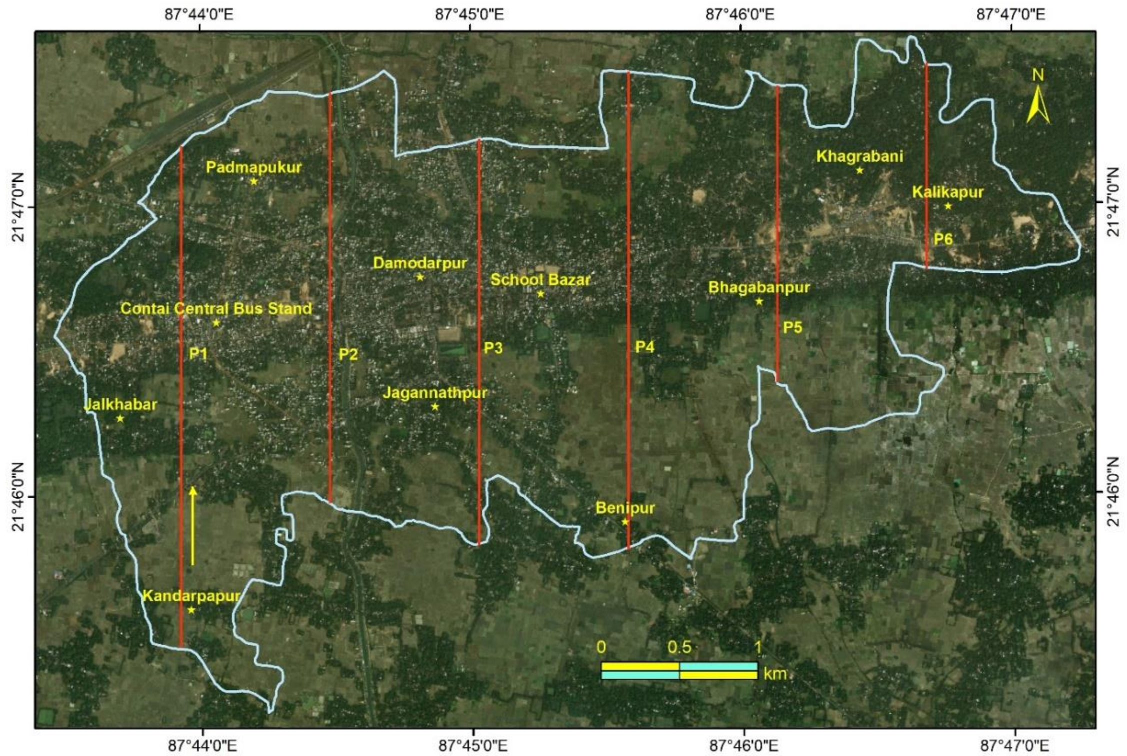

Fig. 4.6: Location of transects across the dune ridges at Contai urban centre.

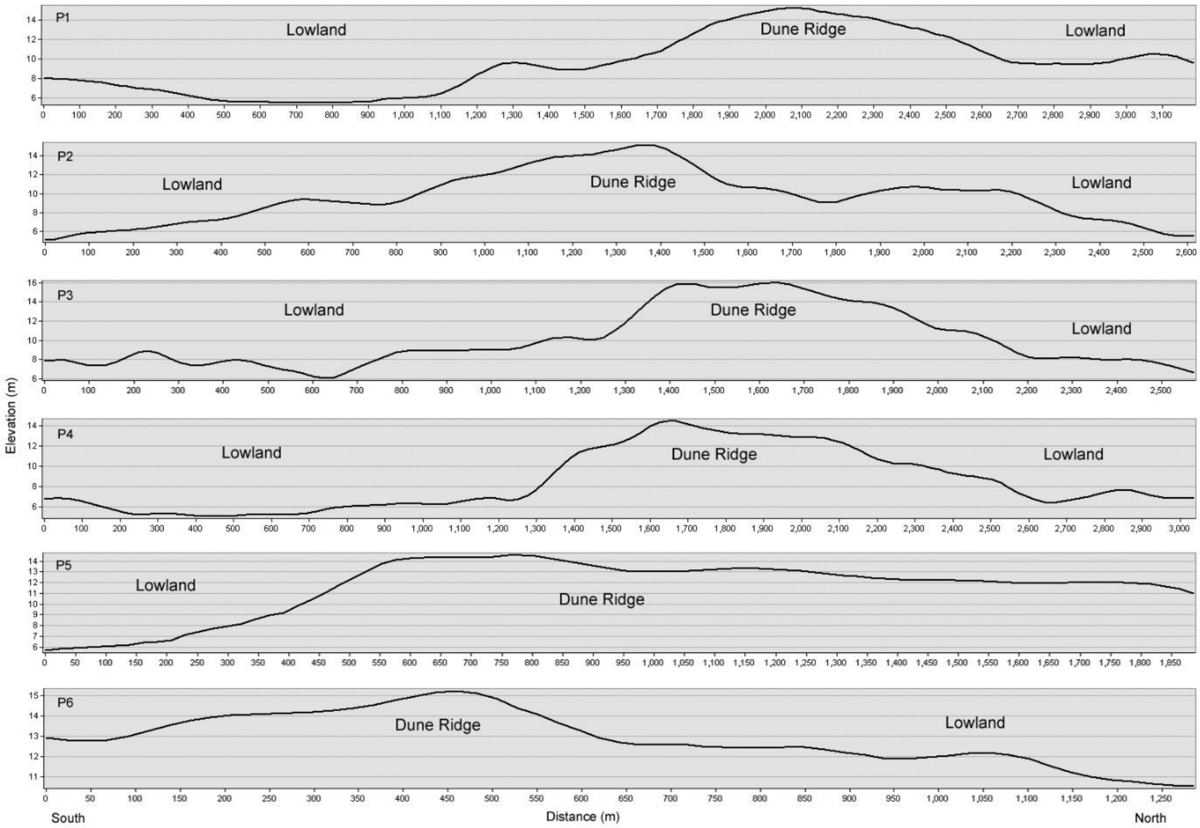

Fig. 4.7: Micro-zonation of surface morphometry along the different transects at Contai.

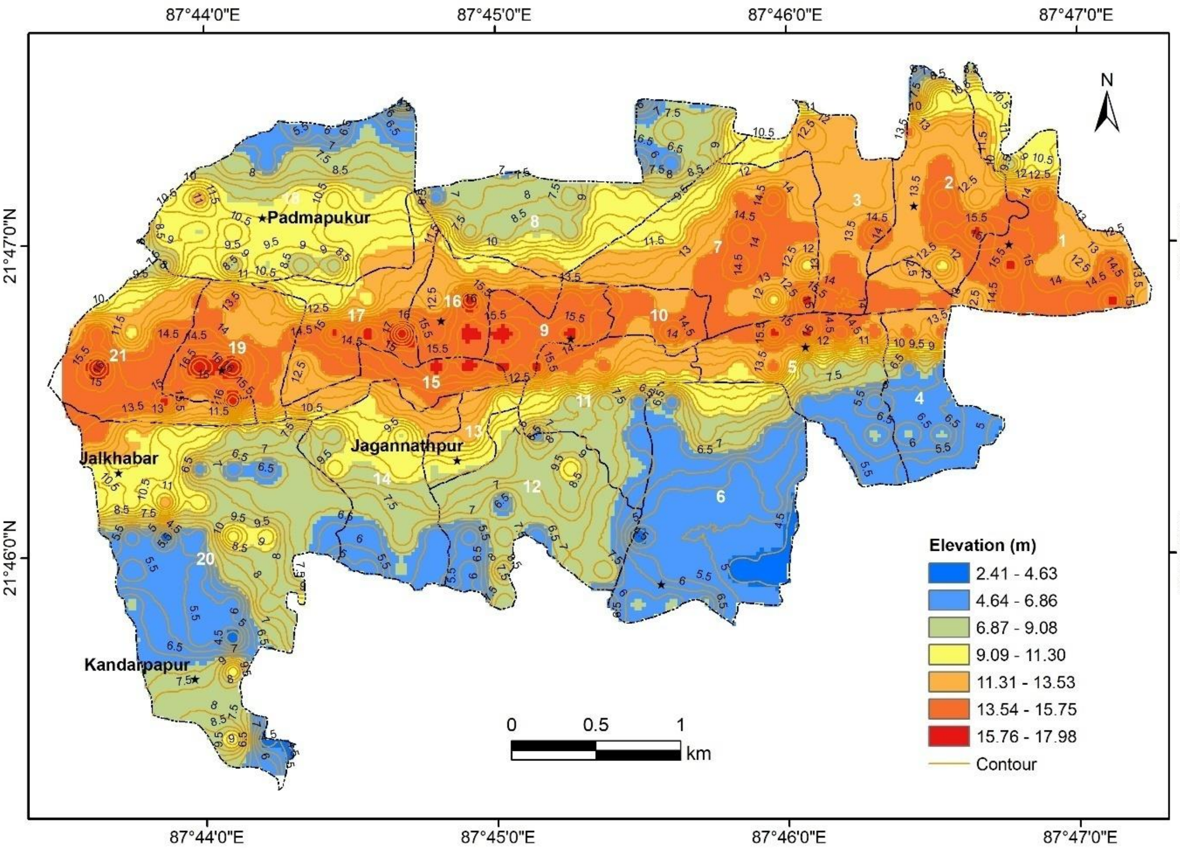

Fig. 4.8: Areas prone to water logging at Contai urban centre.

The lower elevation is observed on both sides of the sand dune and the high slope has been observed at the dune fringes. Micro-level contour pattern and terrain characteristics also confer the relative existence of the dune ridge and lowlands. The storm rainfall (average 1200 mm) in the southwest monsoon months is responsible for water-logging at the low-lying areas. The natural depressions on both sides of the dune are severely affected by water-logging as the rainwater cannot able to drain in the mild sloppy surfaces. There have not observed any significant canals or any natural drainage system to drain such volume of rainwater. During the events of short term intensity of rainfall particularly during cyclone landfalls can produced water logging in the urban fringe areas of Contai. In the year 1997, during the landfall of Contai Cyclone, 495mm of rainfall took place in 48 hours period (Paul, 2002). If such incidence takes place in future with climate change process then the contour areas of 4.44m surface may be affected by a large scale water logging in the Contai municipality areas (that is estimated as 22% area (3.21 km²) of the total area (14.35 km²) (Fig. 4.8). The estimated water-logged areas (Fig. 4.8) mainly utilized for agriculture practices and newly constructed settlement area (Fig. 2.19). Moreover, the recent trends of urban expansion over the low-lying areas can increase more risk and vulnerability for the dwellers in future.

4.2.3. Tidal inundation at Haldia

The Haldia urban centre has existed in the estuary fringe problematic zone. Therefore, tidewater encroachment into the interior part and land inundation will create a severe impact in the faster growing urban-industrial areas. The elevated natural levee has already been embraced with urban-industrial infrastructures. Recently (2019), in the low-lying interior part a new ward has been incorporated with the municipality. Moreover, the exaggerated rate of lowland filling has been observed in the municipality area for construction of the urban infrastructures. The existing tidal channels have also been degraded by landfilling, therefore, the entire land areas in the interior part of the municipality are remained under risk-prone and vulnerable.

The seven (P1 – P7) transects have been demarcated about 2.75 km spatial interval (Fig. 4.9) across the Haldia municipality area. The micro-terrain morphometry reveals the bowl shape lower elevation landscape at the central part of the municipality (Fig. 4.10). The micro-level contour pattern and elevation also confers the bowl or saucer shape landscape (Fig. 4.11). Considering the elevation differences and estuarine tidal environment, the 0.98 m depth of ponding has been considered over the 8.47 m elevated land surface (Fig. 4.11). The rainwater-logging and saltwater inundations will affect about 6.69 km² area (about 17 %) of the total municipality area (99.97 km²). The high-density urban infrastructures, agricultural land and vegetations have existed (Fig. 2.24) within the estimated inundation zones. Therefore, the inundation zone will create more risk and vulnerability in future.

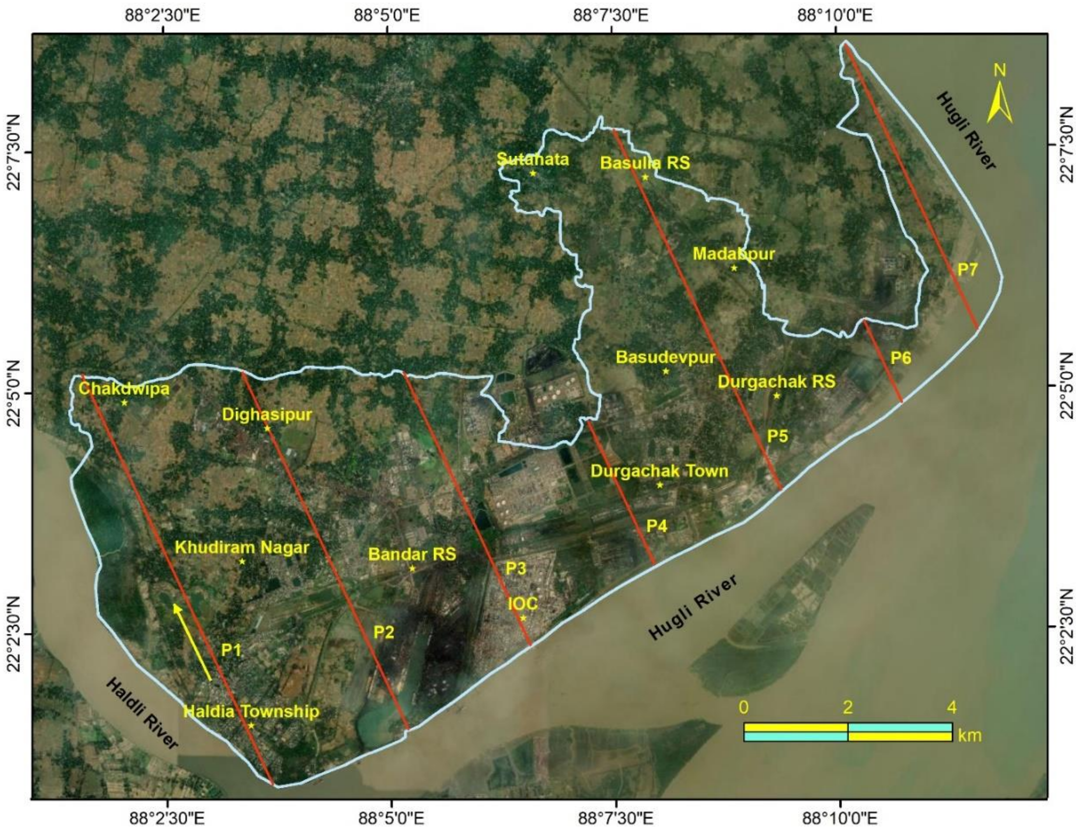

Fig. 4.9: Location of transects across the floodplain-levees at Haldia urban centre.

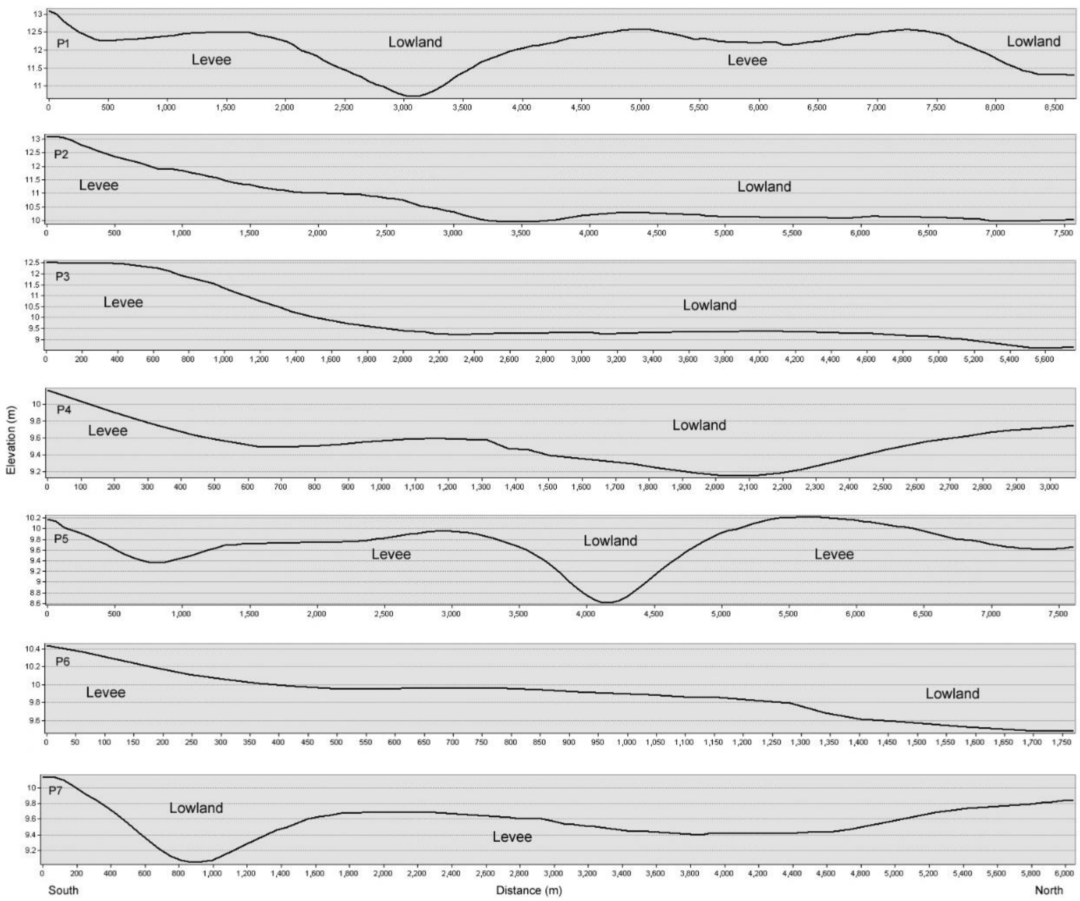

Fig. 4.10: Micro-zonation of surface morphometry along the different transects at Haldia**.**

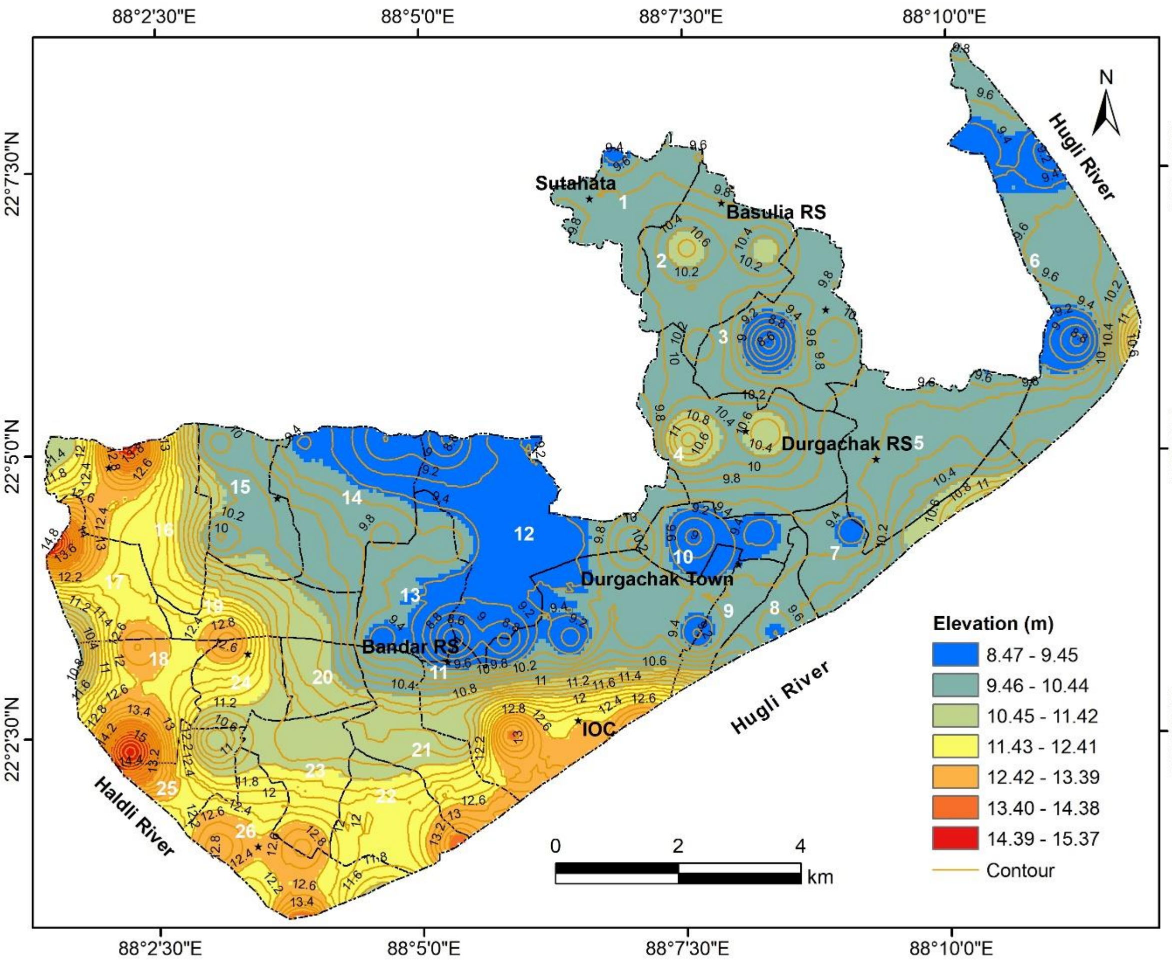

Fig. 4.11: Water logging and saltwater inundation prone areas at Haldia urban centre.

4.3. Cyclonic events and associated risk

The Bengal coast has been affected by about 5–6 cyclones per year (Singh et al., 2001). The long-term trend of the different depressions and cyclonic events reveal that about 1211 cyclones have been formed during 1891 – 2018 in the Bay of Bengal (Cyclone eAtlas, 2019). During 1999, the entire coastal part of Purba Medinipur district has been tremendously affected by the Odisha super cyclone (Kalsi, 2006). Also, the Bengal coast has been affected by the cyclones those provoked the coastal part of Odisha, West Bengal and Bangladesh. The livelihood of the coastal people mainly the fisherfolk and agrarian community have been severely affected by cyclones and associated coastal inundations. The repeated cyclonic events create more vulnerability to the coastal peoples. Therefore, the analysis of the cyclonic trends and distribution in the Bay of Bengal coast has been done in this study.

4.3.1. Intensity of cyclonic events

The month-wise events of Depression (D), Cyclonic Storm (CS), and Severe Cyclonic Storm (SCS) in the Bay of Bengal during 1891-2018 shows that maximum number of cyclonic events have been observed in the pre-monsoon (May), monsoon (July – September) and in the later phase of the monsoon (October – November) (Fig. 4.12; Table 4.1). However, the SCS mainly occurs in the month of May and October – November. The overall trend of D, CS and SCS during 1891 – 2018 reveals that the trends of D (-0.12) and CS (-0.48) have been decreasing, whereas, the trend of SCS has increased at a significant level (0.11) (Fig. 4.12). The study also shows that the overall cyclone frequency has been decreased in the last three decades which is correlated with the earlier results (Mandke & Bhide, 2003; Vishnu et al., 2016). The regional distribution of the number of SCS reveals that the Odisha and West Bengal coasts have been affected by 29 number of SCS during 1891 – 2018 (Fig. 4.13). Whereas, the coastal region of Bangladesh, Tamil Nadu and Andhra Pradesh has been affected by 48, 42 and 44 number of SCS, respectively within this period (Fig. 4.13). The historical cyclone tracks in the Bay of Bengal coast indicate that the frequency (trend) of cyclones is increasing during the post-monsoon phase in compared with the pre-monsoon phase (Srivastava at el., 2000; Sahoo & Bhaskaran, 2016). Also, the increasing SST in the Bay of Bengal leads to escalating the frequency of SCS in the global warming scenario (Jadhav & Munot, 2009; Midya et al., 2019).

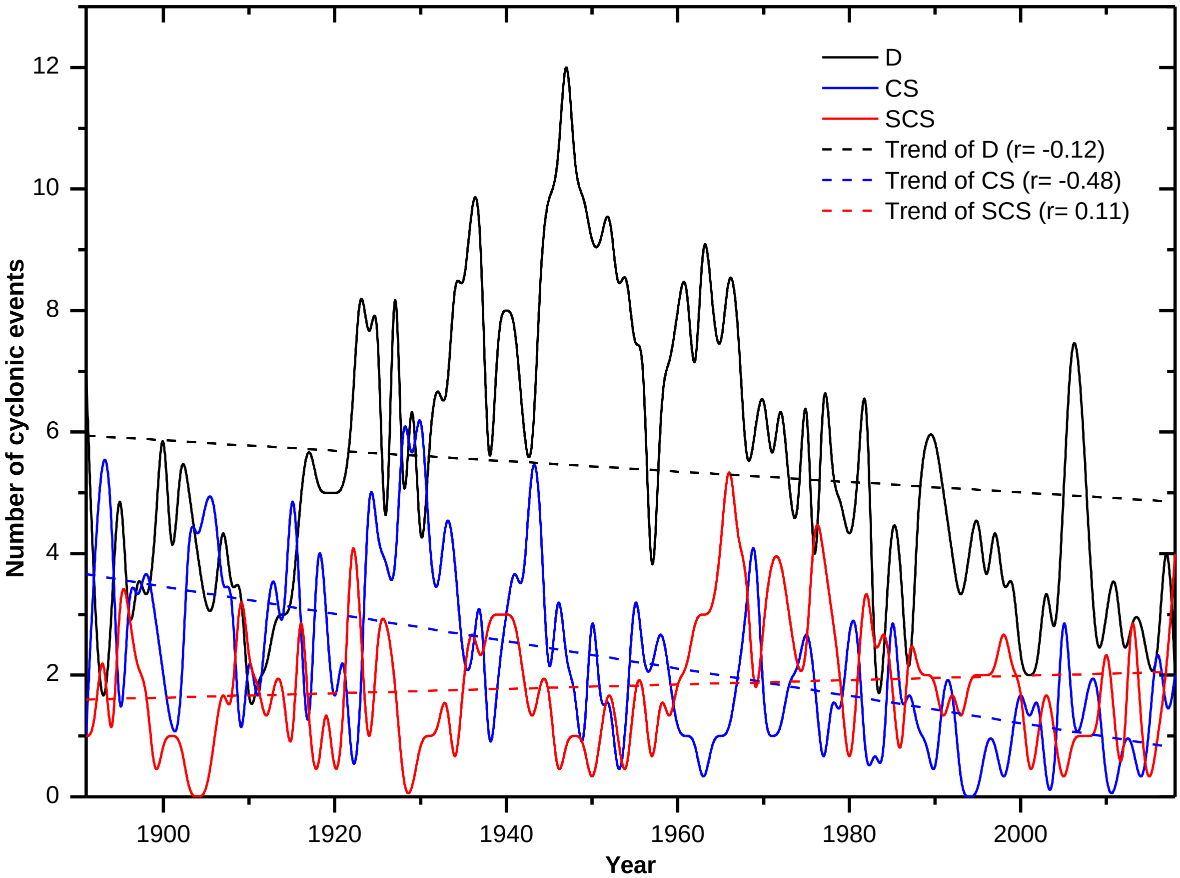

Fig. 4.12: Year-wise cyclonic events of depression (D), cyclonic storm (CS), and severe cyclonic storm (SCS) and their trends in the Bay of Bengal during 1891-2018 (showing the vulnerabilities).

Table 4.1: Monthly and annual frequency of different cyclonic events at the Bay of Bengal during 1891 – 2018 to show the vulnerability status of the coastal belt.

Types of cyclone	Jan	Feb	Mar	Apr	May	Jun	Jul	Aug	Sep	Oct	Nov	Dec	Annual
D+CS+SCS	18	6	7	34	92	112	149	181	166	193	168	85	1211
CS+SCS	7	2	5	27	63	38	43	29	41	92	121	52	520
SCS	2	1	2	14	42	5	8	4	15	42	72	27	234

Depression (D), Cyclonic storm (CS), and Severe cyclonic storm (SCS).

Plate 4.3: Cyclonic storm-wave overtopping the seawall at Digha.

Plate 4.4: Cyclonic storm frequently inundating the new areas of shorefront position at Digha.

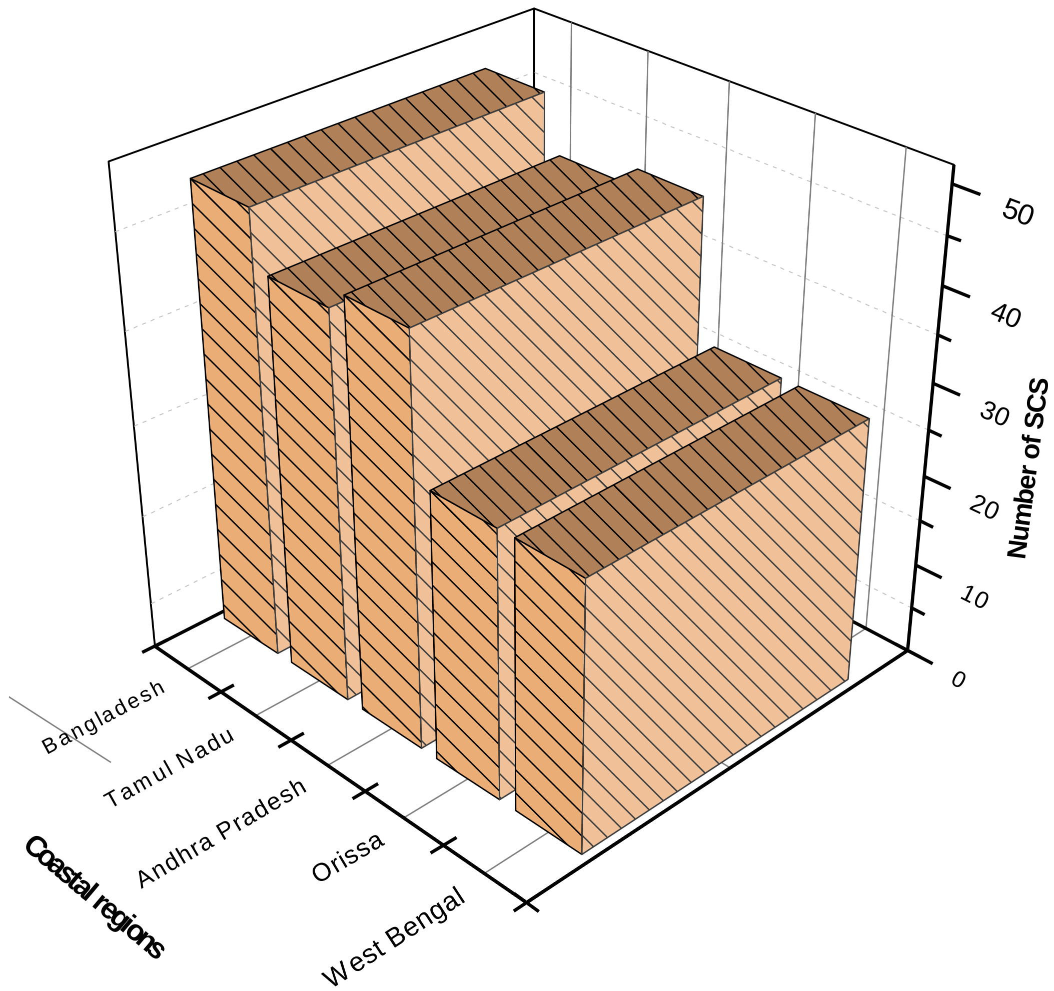

Fig. 4.13: Regional distribution of severe cyclonic storm (SCS) events in the Bay of Bengal coast during 1891 – 2018 (showing the vulnerabilities).

4.3.2. Cyclone track

The overall observation of the cyclone tracks in the Bay of Bengal reveals that most of the post-monsoon cyclonic landfall was happen in the coastal states of West Bengal (20), Odisha (27), Andhra Pradesh (31), and Tamil Nadu (29), which is greater in compared with the pre-monsoon cyclones (Sahoo & Bhaskaran, 2016). The spatial variability in SST and air temperature is not significant during the pre-monsoon period. Therefore, a minimum number of cyclone forms during the pre-monsoon period than the post-monsoon period (Sahoo & Bhaskaran, 2016). The cyclone tracks in the Odisha and West Bengal coasts at the temporal spans of 20 years (Fig. 4.14; Table 4.2) indicates that the highest number (259) of cyclonic events have been observed during 1931 – 1950 (Fig. 4.14c). Although, the number of cyclones is minimum (45) during 2011 – 2018, but these happened only within 8 years (Table 4.2). After the 1970s, the number of cyclonic events has been decreasing (Fig. 4.14e, f; Table 4.2) compared with the previous periods (since 1891 – 1970) (Fig. 4.14; Table 4.2).

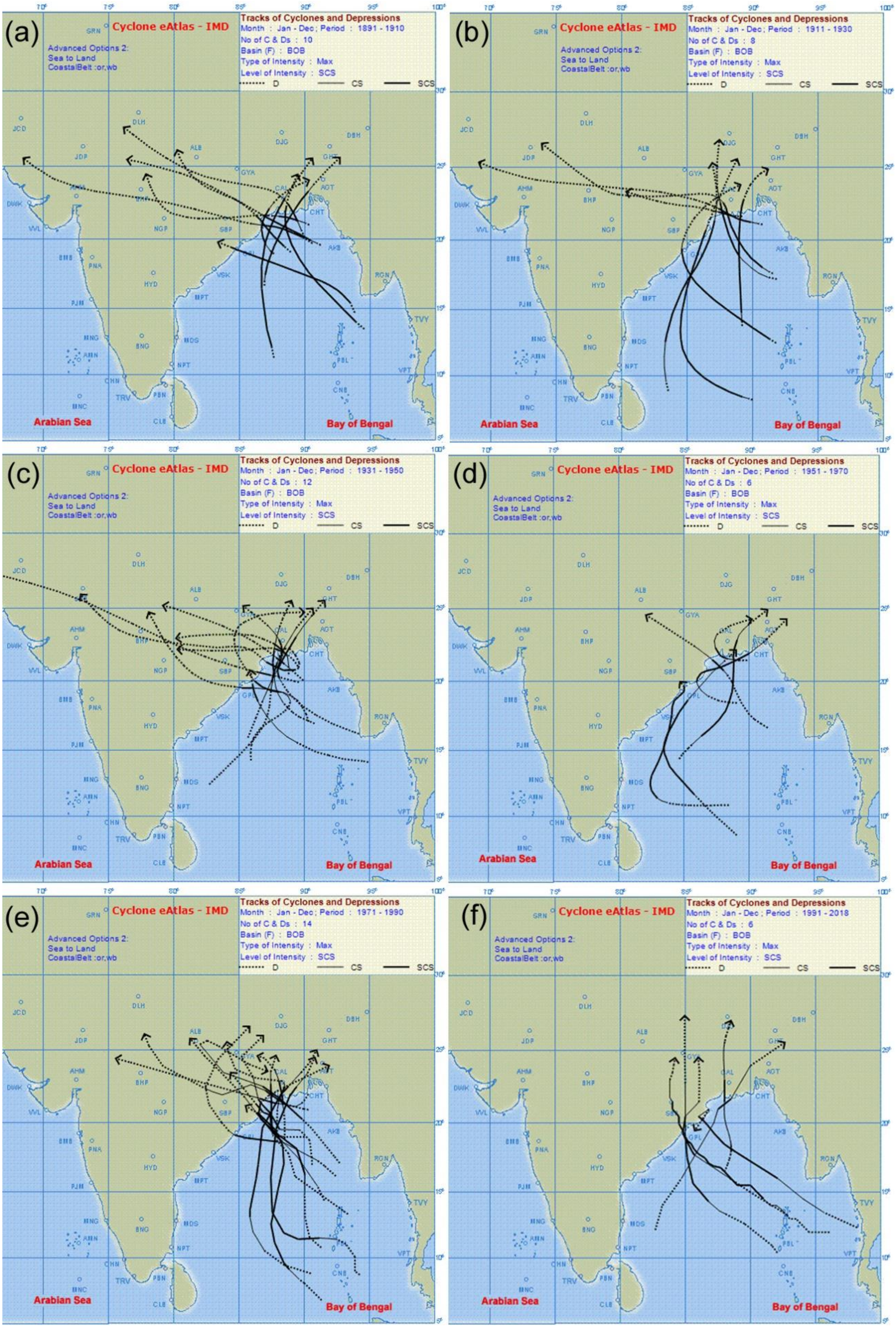

Fig. 4.14: Areas prone to the vulnerabilities resulted from the track of severe cyclonic storm (SCS) within the West Bengal and Odisha coasts during (a) 1891-1910, (b) 1911-1930, (c) 1931-1950, (d) 1951-1970, (e) 1971-1990, and (f) 1991-2018. (Source: Cyclone eAtlas – IMD (http://14.139.191.203/ViewByParam.aspx)

Table 4.2: Periodic frequency of cyclonic events of depression (D), cyclonic storm (CS) and severe cyclonic storm (SCS) in the Bay of Bengal for the span of 128 years.

Period	Cyclone category			
	D	CS	SCS	All
1891 - 1910	77	63	29	169
1911 - 1930	102	68	32	202
1931 - 1950	166	60	33	259
1951 - 1970	150	34	46	230
1971 - 1990	96	30	51	177
1991 - 2010	77	22	30	129
2011 - 2018	23	9	13	45

In the recent context, the coastal region of the study area as well as the West Bengal has been severely affected by the tropical cyclones like Aila (2009), Hudhud (2014), Titli (2017), Phailin (2018), Fani (2019), and Bulbul (2019). The casualty and loss of properties are common aspects with the cyclonic events which intensify the miseries of the coastal people. At the shorefront areas, cyclonic storm surges overtopping the sea-wall at the Digha-Sankarpur coastal zone (Plate 4.3) which creates a severe impact on the local economy and also due to saline water encroachment and stagnant into the natural depression areas (Plate 4.4). Moreover, the densely populated and infrastructurally developed urban areas in the low-lying coastal stretch are prone to additional risk and vulnerability from the immense impact of the frequent tropical cyclones. In the recent era of technological development, it is quite possible to predict the track of a cyclone and their possible site of landfall. Therefore, the necessary precaution and adaptation strategies are possible which can minimize the casualty and loss of wealth in the way to risk reduction.

4.4. Coastal erosion and increasing vulnerability

Since the 1970s, the beach and dune are severely eroded in the Digha-Mandarmani coastal areas (Niyogi, 1970; Paul, 2002; Jana et al., 2014). During 1972 – 2010, about 4 km² areas of coastal land erosion (Jana et al., 2014) is reflected on the area of shorefront mouza like Atili, Gangadharpur, Jagaibasan, Nilpur, Digha, Raypur, Jamra Shyampur, Begundiha, and Kiagoria. Those mouza are shrinking their areas or entirely eroded in respect to the cadastral map (BADP, 2014). In this study, the satellite image of 1973, 1980, 1991, 2001, 2011 and 2018 have been used for the study of shoreline and bankline shifting assessment along the shore and major rivers and tidal inlets (Fig. 4.15). The shoreline areas of the Digha-Mandarmani and Haldia are divided into five major zones of Haldia (north) (9.5 km), Haldia (south) (8.7 km), Mandarmani (13.6 km), Sankarpur-Tajpur (9.3 km), and Digha (6.7 km) coastal stretches (Table 4.3). The Haldia coastal stretch has been divided depending on the erosion and accretion nature of the Hugli river bank (considered as shoreline) in the northern and southern part. The shoreline shifting analysis has been done in the entire coastal stretch from the part of Hugli river at Haldia (north) to Subarnarekha mouth (south). Moreover, the river banks of Hugli, Haldi, Rasulpur, Pichaboni, Jaldah, and Champa are selected for the bank shifting analysis (Fig. 4.15). Only the right bank of the Hugli river is considered for the bank shifting analysis as the Haldia urban centre is located at the right bank of Hugli. However, both banks of Haldi are considered for bank shifting analysis. Other river channels of Pichaboni, Jaldah and Champa are located in the Digha-Mandarmani coastal stretch. Although, the Rasulpur is not a part of the present study area, yet it considered in this study as it is located in the littoral-coastal stretch. In the shoreline and bankline shifting analysis, Net Shoreline Movement (NSM) and Linear Regression Rate (LRR) methods are adopted in the Digital Shoreline Analysis System (DSAS) model. In the study of shoreline and bankline shifting analysis, the negative (-) trend indicates the erosion nature and positive shifting reveals the accretion nature of shifting.

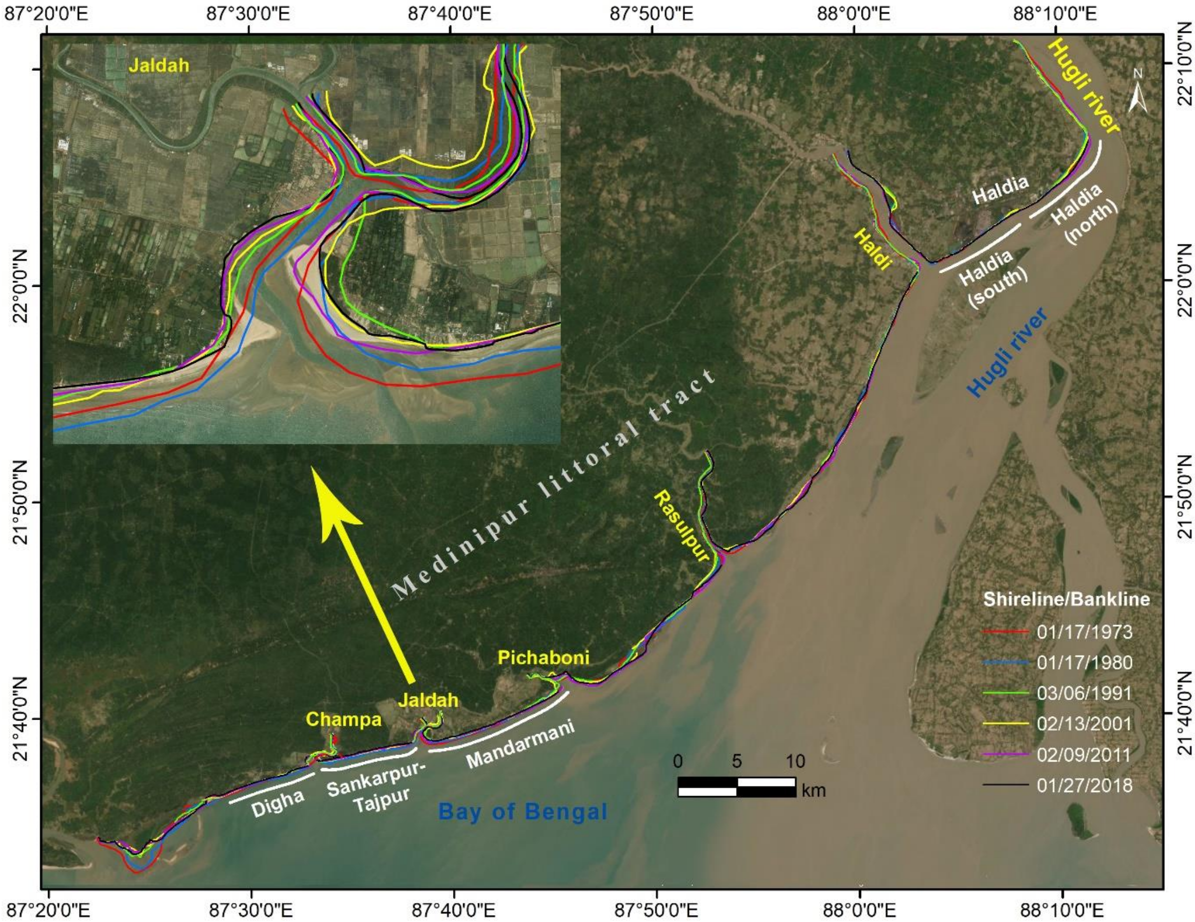

Fig. 4.15: Position of shorelines and banklines during 1973 – 2018 in and around the study area. The positions of banklines along the river Champa, Jaldah, Pichaboni, Rasulpur, Haldi, and Hugli are selected for the bank shifting analysis. The coastal stretches of Digha, Sankarpur-Tajpur, Mandarmani, Haldia (north) and Haldia (south) are selected for detailed shoreline shifting analysis.

4.4.1. Shoreline erosion and shifting

The result of shoreline shifting nature reveals the highest rate of erosion at the mouth of the Subarnarekha river, although this is not a part of the present study (Fig. 4.16, 4.17). The overall shoreline shifting nature divulges that the maximum net erosion (1921.40 m) is resulted at the coastal areas of Subarnarekha river mouth and accretion (856.16 m) at the beach near Soula river mouth (Fig. 4.16) with a maximum erosion and accretion rate of -105.27 m/y and 20.43 m/y, respectively (Fig. 4.17) during 1973 – 2018. However, in the selected coastal stretch (Fig. 4.15), the NSM (Fig. 4.16) shows the erosion at the entire coastal stretch of the Digha and Sankarpur-Tajpur, and western part of the Mandarmani stretch. The Haldia (south) section is also experienced erosion nature (Plate 4.5). Whereas, accretion is observed in the Haldia (north), at the position of recently deposited mud-bank (muddy field) and eastern side (Dakshin Purushottampur) of the Mandarmani coastal stretch. The micro-zone wise shoreline shifting analysis reveals the overall accretion (103.53 m) at the Haldia (north) area and the erosion in

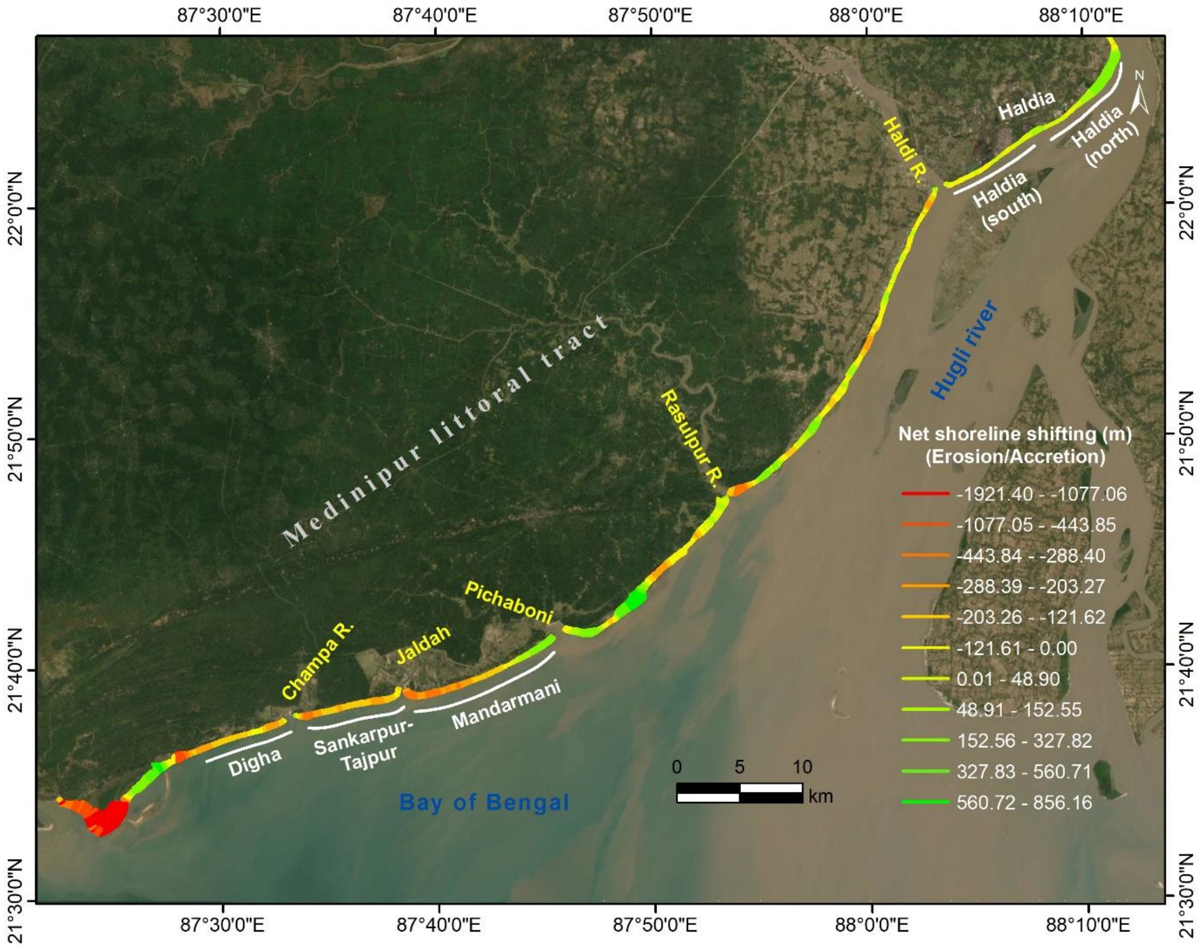

Fig. 4.16: Distance of Net Shoreline Movement (NSM) along the coastal stretch of Digha, Shankarpur-Tajpur, Mandarmani, and Haldia during 1973 – 2018. Transects are superposed over the recent image (2019).

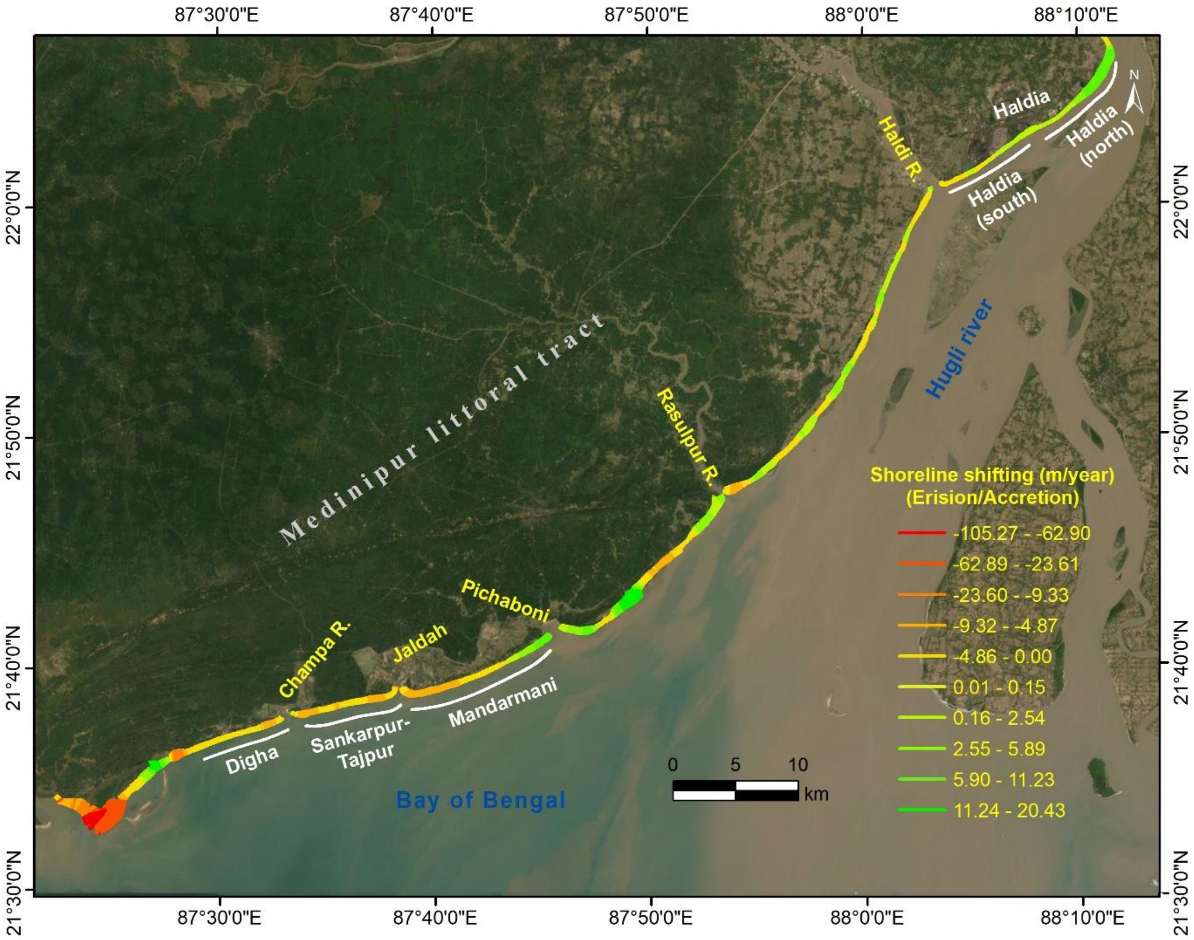

Fig. 4.17: Linear Regression Rate (LRR) of shoreline shifting and resultant erosion-accretion along the shoreline of Digha, Shankarpur-Tajpur, Mandarmani, and Haldia coastal stretch during 1973 – 2018. Transects are superposed over the recent image (2019).

the rest of the areas (Table 4.3). At Digha, only the erosion nature of shoreline shifting is resulted, whereas, in the rest of the stretches the erosion and accretion nature are observed (Table 4.3). Among the five coastal stretches (Table 4.3), the maximum (393.40 m) and minimum (0.09 m) net erosion are observed at the Sankarpur-Tajpur and Haldia (south) area respectively. These two sites also experienced with the maximum (-8.86 m/y) and minimum (-0.02 m/y) negative rate (erosion) shoreline shifting (Table 4.3). Whereas, the maximum (423.88 m) and minimum (0.39 m) accretion are observed at Haldia (south). The maximum (9.60 m/y) and minimum (0.03 m/y) rate of positive shoreline shifting (accretion) resulted at Haldia (north) and Sankarpur-Tajpur coastal stretch. Also, the micro-zone wise estimation of mean erosion and accretion nature of shoreline confers the greater erosion than accretion along the zone of Digha, Sankarpur-Tajpur, and Haldia (south), whereas, just reverse shoreline shifting nature at Mandarmani and Haldia (north) coastal stretch (Table 4.3). The other detail status (mean, maximum and minimum erosion and accretion nature) of the zone-wise net (NSM) and rate (LRR) of shoreline shifting are mentioned in Table 4.3. The overall rate of shoreline shifting within the coastal stretch of the Hugli river (north) to Subarnarekha river mouth (South) reveals the erosion trend (-0.36) (Fig. 4.18).

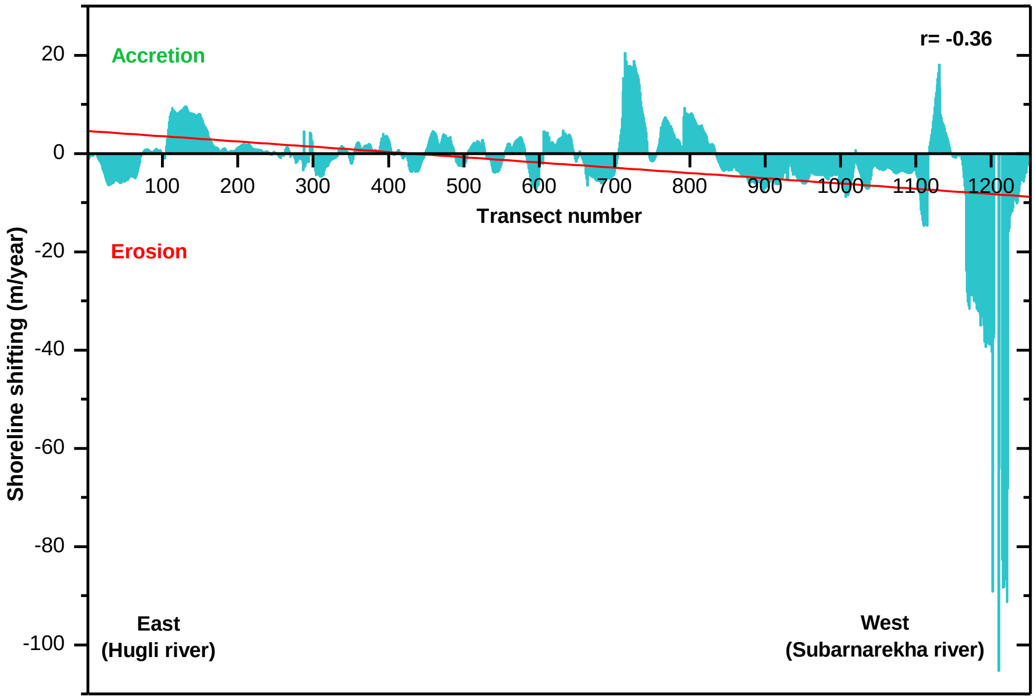

Fig. 4.18: Transect wise shoreline shifting rate and resultant erosion-accretion in and around the study area of Medinipur littoral tract during 1973 – 2018.

4.4.2. Riverbank erosion and shifting

Likewise the shoreline shifting, the bankline shifting nature has been assessed for both banks (except Hugli) of the selected rivers (Fig. 4.15). The NSM indicates that net shifting of bankline and LRR reveals the rate of bank shifting during 1973 – 2018. The NSM based net bankline shifting divulges the maximum erosion (900.07 m) and accretion (718.32 m) within the entire river banks (Fig. 4.19), whereas, the maximum rate of shifting varies from -28.24 m/y to 31.61 m/y (Fig. 4.20). Depending on the curvature of the flow paths within the selected area, the length of the banklines (left and right) varies i.e. the length of the left and right bank of Pichaboni (Fig. 4.19, 4.20) are 4.90 km and 4.20 km respectively (Table 4.4). Therefore, the number of transects also vary accordingly. The NSM and LRR based overall mean (erosion-accretion) and mean, maximum and minimum erosion or accretion has been estimated for both banks (for Hugli, only the right bank) of the rivers (Table 4.4). The estimated bank-wise overall mean shifting nature (net bankline shifting) reveals the erosion at the right bank of Hugli, Haldi, and Champa, and at the left bank of Rasulpur, Pichaboni and Jaldah, whereas, the deposition nature is observed on the opposite banks (Table 4.4). However, the rate of shifting is not in similar nature with the net shifting. The positive (accretionary) trend is observed along the right banks of Hugli, Rasulpur and Pichaboni, and in the left banks of Haldi and Champa. The negative (erosional) trend is observed in the right banks of Haldi, Jaldah and Champa, and in the left banks of Rasulpur, Pichaboni and Jaldah. In case of the Jaldah river, the left (-3.31 m/y) and right (-0.58 m/y) banks have resulted with the erosional trend, otherwise, the rest of the banks experienced with either erosion or deposition on the left of right bank (Table 4.4). The significant level of accretion is observed at the left bank of the river Haldi where mangrove vegetations are grown (Plate 2.7) at ward number 17 (Fig. 2.20).

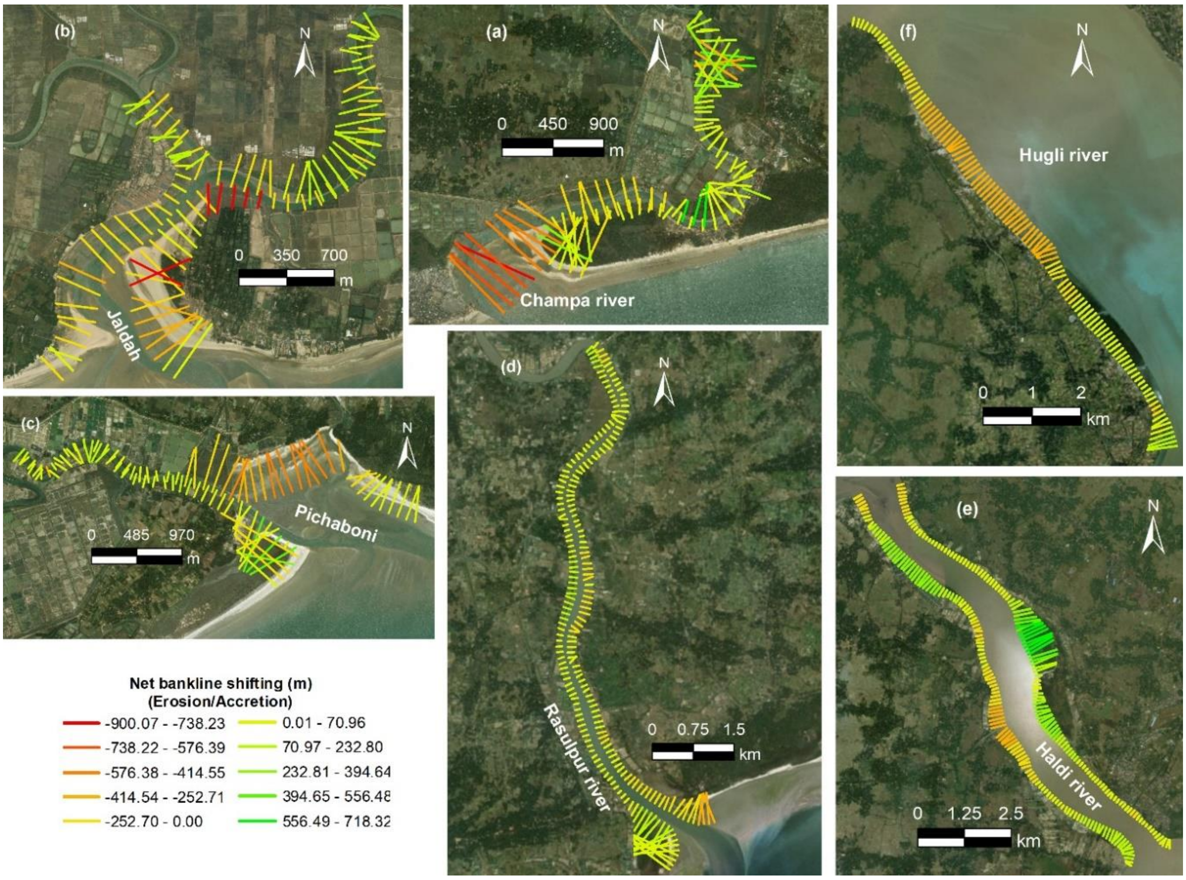

Fig. 4.19: Distance of net bankline movement during 1973 – 2018 along the (a) Champa river, (b) Jaldah inlet, (c) Pichaboni inlet, (d) Rasulpur river, (e) Haldi river, and (f) right bank of Hugli river under the present littoral tract. Transects are superposed over the recent image (2019).

Plate 4.5: Mud-bank erosion at the right bank of Hugli river in Haldia.

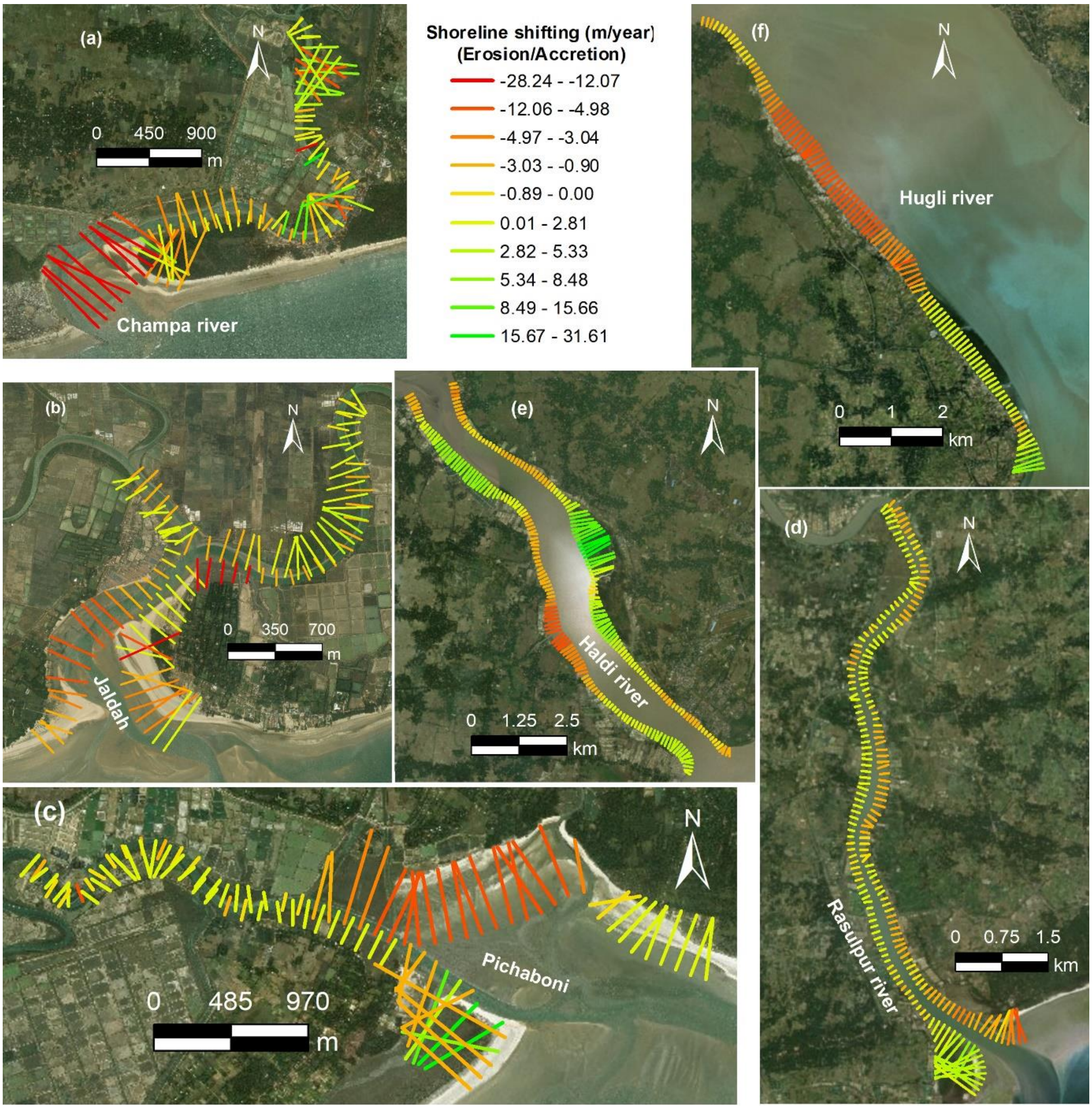

Fig. 4.20: Linear Regression Rate (LRR) of bankline shifting and resultant erosion-accretion along the banks of (a) Champa river, (b) Jaldah inlet, (c) Pichaboni inlet, (d) Rasulpur river, (e) Haldi river, and (f) right bank of Hugli river during 1973 – 2018. Transects are superposed over the recent image (2019).

At the coastal stretch of Digha and Sankarpur-Tajpur (particularly at the mouth of Champa river), the severe shoreline (Fig. 4.16, 4.17, 4.21; Table 4.3) and bankline (Fig. 4.19a, 4.20a; Table 4.4) erosion is responsible for entire erosion of the mouza (Begundiha, and Kiagoria), those currently remains under the seawater (BADP, 2014). Also, the mouza areas of Atili, Digha, Gangadharpur and Jagaibasan are severely eroded and shrank due to erosion (Fig. 4.21). The census year-wise population distribution (Table 3.1) reveals that those mouza are mostly depopulated or population gradually reduced during 1991 – 2011.

Table 4.3: Net Shoreline Movement (NSM) and Linear Regression Rate (LRR) model-derived shoreline shifting nature (erosion and accretion) along the sections of Medinipur coast.

Coastal stretch	NSM (m)					LRR (m/y)				
	Digha	Sankarpur-Tajpur	Mandarmani	Haldia (south)	Haldia (North)	Digha	Sankarpur-Tajpur	Mandarmani	Haldia (south)	Haldia (North)
Length of coastline (km)*	6.70	9.30	13.60	8.70	9.50	6.70	9.30	13.60	8.70	9.50
No. of transects**	67	93	136	87	95	67	93	136	87	95
Overall mean (erosion/accretion)	-173.86	-190.00	-111.46	-8.42	103.53	-3.86	-4.84	-1.52	0.06	4.46
Mean erosion	-173.86	-195.19	-139.02	-39.54	-15.23	-3.86	-4.95	-4.62	-1.01	NA
Maximum erosion	-277.10	-393.40	-378.87	-105.74	-29.42	-7.19	-8.86	-7.62	-3.40	NA
Minimum erosion	-23.54	-2.26	-1.61	-0.09	-0.80	-1.26	-1.78	-0.33	-0.02	NA
Mean accretion	NA	46.22	184.13	26.50	112.97	NA	0.36	5.18	0.87	4.51
Maximum accretion	NA	85.82	319.55	423.88	239.03	NA	0.72	9.28	4.45	9.60
Minimum accretion	NA	6.62	13.94	0.39	0.48	NA	0.01	0.18	0.03	0.05

*Note: The units of * (length of coastline) & ** (No. of transects) in row are not applicable for the measurement units of NSM and LRR. 'NA' assigned where the erosion or accretion is not found.*

Table 4.4: Net Shoreline Movement (NSM) and Linear Regression Rate (LRR) model-derived bankline shifting nature (erosion and accretion) along the different river banks in the Medinipur littoral tract.

Bank shifting nature	River banks	NSM (m)						LRR (m/y)					
		Hugli	Haldi	Rasulpur	Pichaboni	Jaldah	Champa	Hugli	Haldi	Rasulpur	Pichaboni	Jaldah	Champa
Length of bankline (km)*	Left	NA	8.10	10.80	4.90	5.10	4.10	NA	8.10	10.80	4.90	5.10	4.10
	Right	5.10	9.50	11.10	4.20	5.50	4.70	5.10	9.50	11.10	4.20	5.50	4.70
No. of transects**	Left	NA	81	108	49	51	41	81.00	NA	108	49	51	41
	Right	51	95	111	42	55	47	51	95	111	42	55	47
Overall mean (erosion/accretion)	Left	NA	168.70	-79.84	-148.51	-184.17	61.36	NA	3.86	-1.15	-2.39	-3.31	0.93
	Right	-72.69	-57.32	38.76	67.72	11.00	-104.17	0.47	-0.60	1.01	2.15	-0.58	-2.60
Mean erosion	Left	NA	-37.51	-93.83	-207.51	-258.73	-48.62	NA	-0.73	-1.16	-4.27	-5.71	-1.52
	Right	-100.67	-153.92	-17.37	-62.61	-109.61	-318.23	-2.25	-3.00	-0.52	-1.24	-2.73	-5.98
Maximum erosion	Left	NA	-99.14	-404.61	-451.54	-900.07	-177.38	NA	-1.70	-6.13	-10.01	-28.24	-4.41
	Right	-317.52	-332.43	-39.66	-173.81	-54.63	-900.07	-5.06	-6.39	-1.28	-2.22	-6.65	-16.58
Minimum erosion	Left	NA	-1.41	-3.32	-3.49	-6.09	-2.22	NA	-0.05	-0.04	-0.01	-0.27	-0.09
	Right	-2.59	-4.82	-2.99	-0.67	-13.80	-16.15	-0.10	-0.04	-0.04	-0.04	-0.19	-0.09
Mean accretion	Left	NA	249.83	32.08	33.38	58.15	139.26	NA	6.98	0.71	1.14	1.47	2.49
	Right	88.82	81.38	50.35	108.45	88.08	184.81	1.65	2.69	1.56	3.63	1.39	5.77
Maximum accretion	Left	NA	718.32	64.27	62.94	122.36	434.36	NA	31.61	1.52	2.65	2.30	7.09
	Right	171.69	150.80	180.16	517.37	218.92	718.32	8.48	5.33	7.12	31.61	3.85	15.66
Minimum accretion	Left	NA	1.63	7.64	3.19	2.78	4.72	NA	0.10	0.01	0.08	0.07	0.02
	Right	2.25	9.06	2.37	16.18	2.61	2.81	0.03	0.14	0.03	0.16	0.19	0.08

*Note: The units of * (length of bankline) & ** (No. of transects) in row are not applicable for the measurement units of NSM and LRR. The left bank of Hugli is not considered in this study is mentioned by 'NA' in the table.*

4.4.3. Beach and dune erosion

The status of beach width is also synchronized with the result of shoreline shifting. At the different coastal sites of Dattapur, Gangadharpur, Jhamra Shyampur, Sankarpur, Chandpur, Jaldah, Tajpur and Mandarmani the beach width is gradually decreasing during the selected periods of 2006, 2012 and 2018 (Fig. 4.22). It is observed that during 2006 – 2012, the shoreline erosion and adjusted beach width has not been significantly changed in compared with the change during 2012 – 2018. In the Mandarmani and Tajpur sites, a prominent trend of beach erosion is observed due to vertical erosion and removal of beach sand which leads to exposure of the mud layer at the beach (Plate 4.6). At that section, the overall shoreline erosion is also higher (Table 4.3). The similar condition is observed at the Sankarpur-Tajpur coastal area where the higher trend of net shoreline retreat (Fig. 4.16) and rate of shifting (Fig. 4.17) is responsible for shoreline (Fig. 4.21) associated with beach erosion (Fig. 4.22).

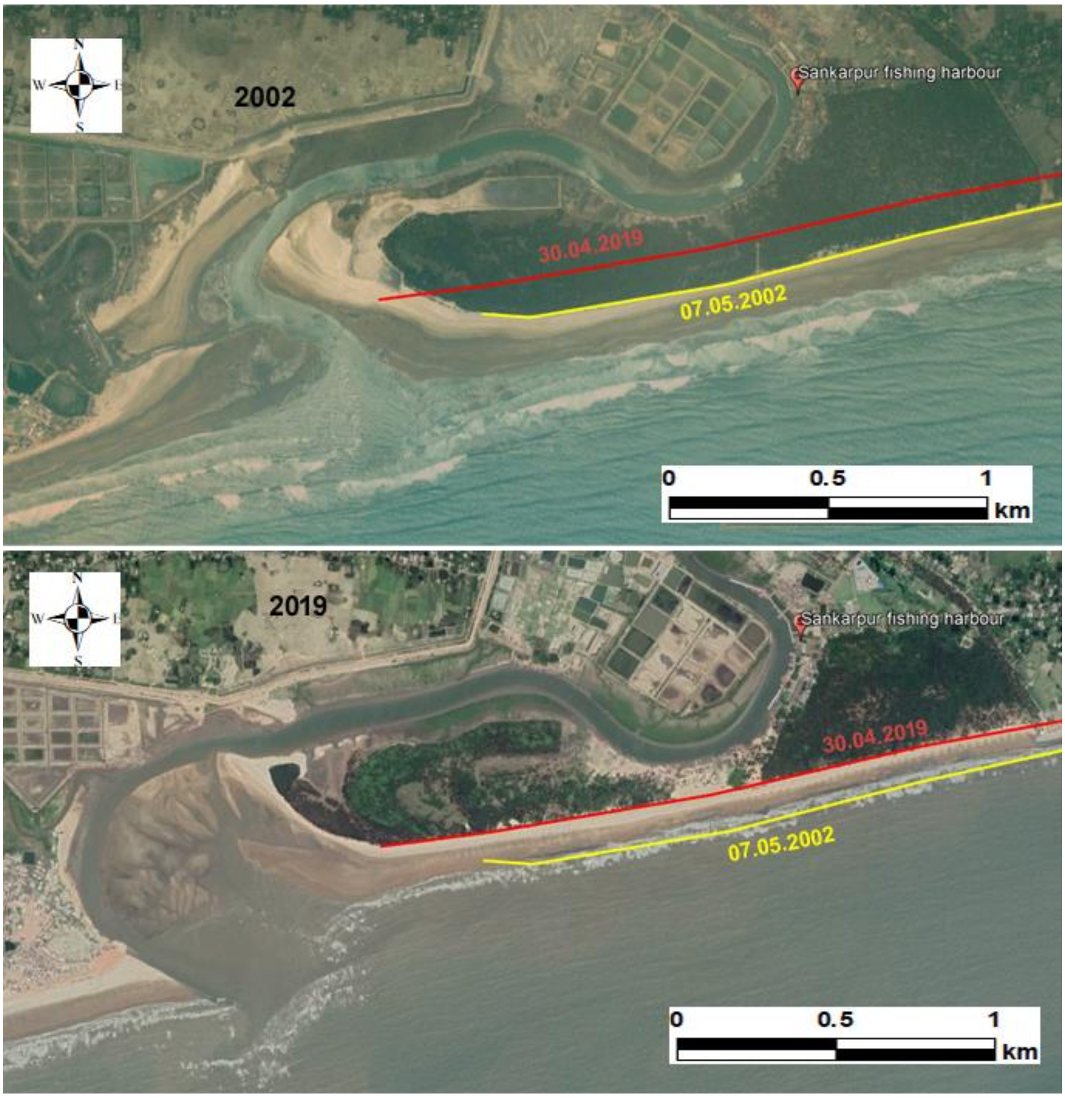

Fig. 4.21: Severe nature of shoreline and bankline erosion at the Champa river mouth (Digha-Sankarpur) during 2002 – 2019.

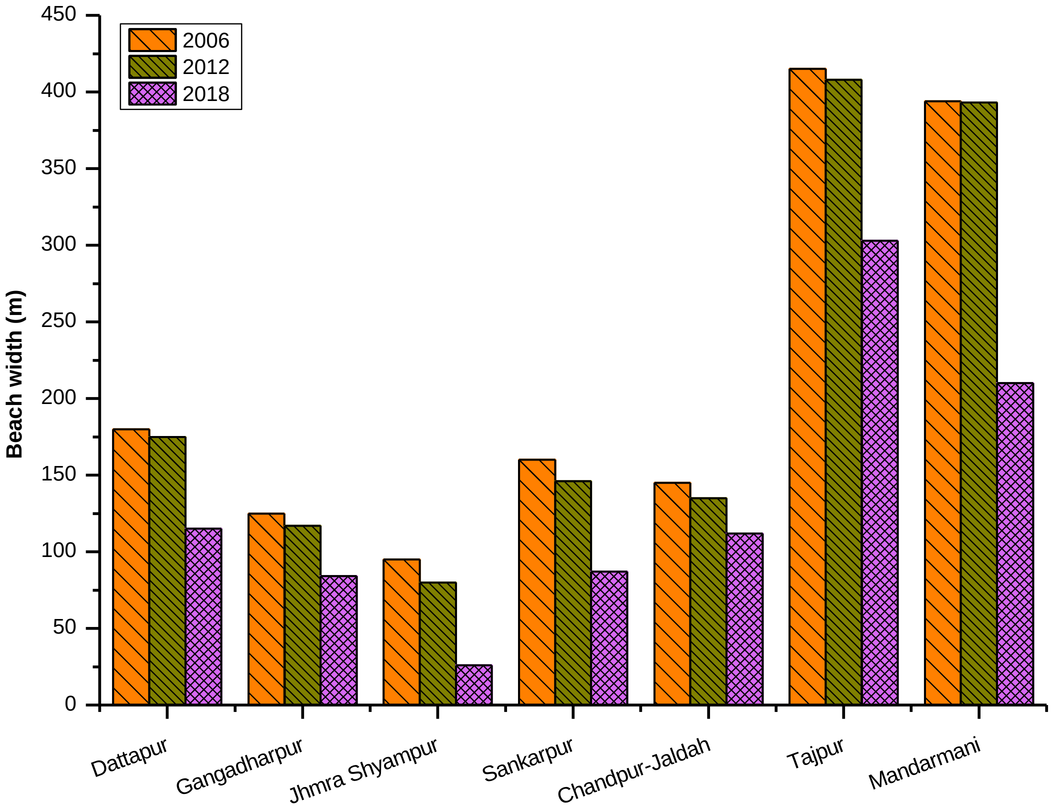

Fig. 4.22: Shoreline erosion and associated beach width reduction at the different coastal stretch during 2006 – 2018.

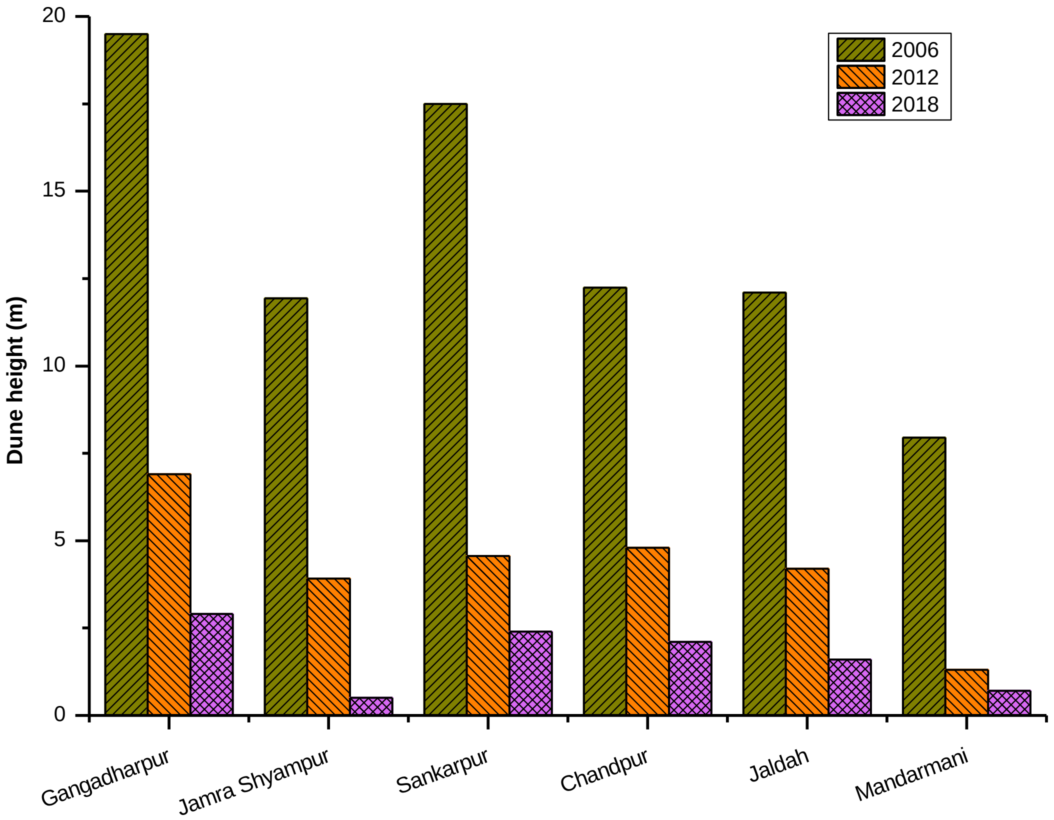

Fig. 4.23: Gradual dune erosion and related reduction of dune elevation at the different coastal parts during 2006 – 2018.

Plate 4.6: Mud layer exposed at (a) Mandarmani and (b) Tajpur coastal belt due to the removal of beach sand by longshore current transport.

Plate 4.7: Some fragmented sand dunes still remain at the shorefront areas of (a) Jamra Shyampur and (b) Mandarmani in unaffected and partially affected conditions.

The elevation of shorefront dunes is highly reduced due to severe rate of dune erosion. As per the field observations during 2006 – 2018, about more than 10 m elevated dunes (2006) have remained as only about 1.5 m height in recent time (2018) (Fig. 4.23). At the site of Jamra Shyampur and Mandarmani, only a few fragmented dune ridges exist (Plate 4.7) with an average height of 0.5 m and 0.7 m, respectively (Fig. 4.23) along the shoreline and most of these are severely eroded. However, some dune ridges have existed at Digha coastal stretch, and most of those are highly degraded due to constructions of tourism infrastructures over the dune landscape after dune cutting and flattening of dune landscape (Plate 2.3, 2.10).

4.5. Major findings

The following major outcomes are found in this chapter.

1. The tide level is increasing at all the stations around the Medinipur coast which can create water-logging and inundation problem (particularly in Haldia).
2. The number of cyclonic events (D, CS and SCS) is decreased, but the trend of SCS is increasing in recent decades.

3. The shoreline is retreating (erosion) at Digha, Mandarmani and western part of Haldia; whereas, sediment accretion is observed at the eastern part (mud-bank) of Haldia. The beach width and dune elevation are significantly decreased all along the Digha-Sankarpur-Mandarmani coastal stretch.